HAL
open science

MODELING OF POWER SEMICONDUCTORS IN VHDL-AMS FOR EMI SIMULATIONS

Slim Hrigua, Cyrille Gautier, Bertrand Revol, François Costa

To cite this version:

Slim Hrigua, Cyrille Gautier, Bertrand Revol, François Costa. MODELING OF POWER SEMICONDUCTORS IN VHDL-AMS FOR EMI SIMULATIONS. ELECTRIMACS 2011, Jun 2011, Paris, France. hal-00623285

HAL Id: hal-00623285

https://hal.science/hal-00623285v1

Submitted on 14 Sep 2011

HAL is a multi-disciplinary open access archive for the deposit and dissemination of scientific research documents, whether they are published or not. The documents may come from teaching and research institutions in France or abroad, or from public or private research centers.

L'archive ouverte pluridisciplinaire **HAL**, est destinée au dépôt et à la diffusion de documents scientifiques de niveau recherche, publiés ou non, émanant des établissements d'enseignement et de recherche français ou étrangers, des laboratoires publics ou privés.

MODELING OF POWER SEMICONDUCTORS IN VHDL-AMS FOR EMI SIMULATIONS

Slim Hrigua[1], Cyrille Gautier[2], Bertrand Revol[1], François Costa[3]

1. SATIE, ENS CACHAN, 61 avenue de Président Wilson, F-94235 Cachan cedex, France.
E-mail: Slim.Hrigua@satie.ens-cachan.fr
2. IUT de Ville d'Avray, Paris 10 University, 50 Rue de Sèvres, F-92410 Ville d'Avray, France.
3. IUFM de Créteil, Paris-Est Créteil University, Place du 8 mai, F-93000 St Denis, France.

Abstract - The static converters are important sources of EMI. In order to reproduce the converters functioning by simulation, a special effort must be provided for the silicon component modeling. In our survey case, these models must be well adapted to the static converters simulation for EMC characterization. In this paper, we have focused on the semiconductor models by providing an IGBT VHDL-AMS model. This work allowed us to evaluate the switching effect on the conducted perturbations in the static converters while keeping a good compromise of accuracy and simulation time.

Keywords – Power components, VHDL-AMS modeling, EMI simulation.

1. NOMENCLATURE

- Ads: Body region area [m^2].
- Agd: Gate-drain overlap area [m^2].
- $b=\mu_n/\mu_p$: Ambipolar mobility ratio [-].
- Ccer: Collector-emitter redistribution capacitance [F].
- Cds: Drain-source depletion capacitance [F].
- Cgd: Gate-drain capacitance [F].
- Cgdj: Gate-drain overlap depletion capacitance [F].
- Cgs: Gate-source capacitance [F].
- Coxd: Gate-drain overlap oxide capacitance [F].
- Coxs: Exceeding oxide capacity [F].
- Dp: Hole diffusivity [$m^2.s^{-1}$].
- Ibss: Steady-state base current [A].
- Iceb: Emitter-base capacitor current [A].
- Iccer: Collector-emitter redistribution current [A].
- Icss: Steady-state collector current [A].
- I_{sne}: Emitter electron saturation current [A].
- I_T: Anode current [A].
- n_i: Intrinsic carrier concentration [m^{-3}].
- Nscl: Collector-base space charge concentration [m^{-3}].
- q: Electronic charge [C].
- Q: Instantaneous excess carrier base charge [C].
- Q_B: Background mobile carrier base charge [C].
- Vds: Drain-source voltage [V].
- Vec: Emitter-collector voltage [V].
- Vgs: Gate-source voltage [V].
- V_{Td}: Gate-drain overlap depletion threshold voltage [V].
- W: Quasi-neutral base width [m].
- Wdsj: Drain-source depletion width [m].
- Wgdj: Gate-drain overlap depletion width [m].
- ε_{si}: Silicon permittivity [F/m].
- τ_{HL}: Base high-level lifetime [s].

2. INTRODUCTION

The simulation of power converter functioning can be done according to increasing levels of complexity depending on the represented phenomena. In the EMC oriented simulation case, it requires precise electric models for all elements that contribute in the converter functioning. Furthermore, the necessity to represent accurately the commutation phenomena over several switching periods leads to significant simulation time. All these elements require a compromise between model complexity and accuracy in order to keep a reasonable simulation time.

Since the semiconductor components switching are the main EMI sources, their models must be able to represent them with a high precision.

In this work, we are going to propose a dynamic IGBT model in VHDL-AMS. The IGBT referenced IRGPC40UD is chosen to establish the model. It integrates an n-channel IGBT chip as well as a fast recovery anti-parallel diode. Some simplifications will be added to the original IGBT model in order to reduce the simulation time. Afterward, both of these models will be implemented in a buck converter in order to observe the evolution of the conducted EMI.

3. VHDL-AMS MODELING

As an on-set of VHDL, VHDL-AMS adds simultaneous instructions permitting to affect, in continuous time, the values transported by the objects 'QUANTITY'. It also provides the object 'TERMINAL' that is considered as a node and

associated to a 'NATURE' that defines its physical domain.

The VHDL-AMS offers the possibility to insert equations descended from physical studies as simultaneous instructions while giving the possibility to introduce some imperfections on the parameters to evaluate their influences on the model performances. Thanks to this multi-abstractions approach, the VHDL-AMS puts at stake several physical domains in low and high-level models and allows regrouping them in a global model having a structural approach. These properties permit to reduce the computing time while detailing some part more finely, whereas others can be modeled in a more abstract manner. All the modeling works in this paper are done using the VHDL-AMS programming language.

4. LUMPED-CHARGE DIODE MODEL

Based on a physical approach, the lumped charge modeling technique leads to a considerable reduction of model complexity while maintaining the internal carrier transport process of the power semiconductor device. Several applications of this technique show good results in literature [2]-[3]. We referred for this work to the Ma-Laurizen diode model [4]. This model was developed to have a better representation of the forward and reverse recovery. The Inclusion of these phenomena is critical in the power converters design and for the simulation of the conducted EMI.

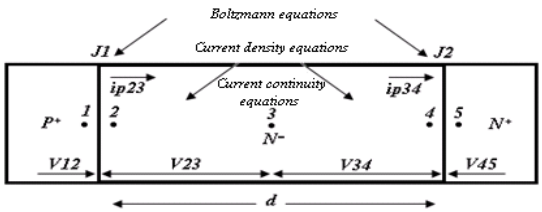

Fig. 1. Lumped-charge distribution in a 1-D $P^+N^-N^+$ diode structure [4].

Thanks to this technique, the basic semiconductor equations are simplified while using a nodal arrangement (Fig. 1). These relations are transformed in lumped-charge equations for every region. In fact, since the weakly doped zone N^- stores the carriers in excess that determines the diode transient features, three nodes (2, 3 and 4) are chosen for this region. The nodes 2 and 4 are connection nodes and the node 3 is the charge storage node. For the highly doped regions, only one node is sufficient to act at the same time as connection and storage charge node. This is due to the weak spatial variations of the carriers concentration. The nodes 1 and 5 are considered sufficient for the N^+ and the P^+ regions.

With regard to the VHDL-AMS diode model, we leaned on the described models in [5] used on SABER simulator. A test circuit, described in the literature [6], was used to evaluate the inverse transient characteristic of the diode model from a null forward current. In the coming works, we will use this diode model in a DC-DC converter as a freewheeling diode.

5. IGBT DYNAMIC MODEL

Up to now, an interval still exists between the industrial development and the valid models on the simulators. As for the IGBT modeling, there is a compromise between the accurateness and the model simplicity. Different approaches exist at the IGBT modeling time, offering for each its own performances to retranscribe at best the real behavior of the device. Departing from this idea, we are trying to pursue these recent efforts by understanding the internal mechanism in order to identify the relevant parameter of the device for the EMI analysis.

For these IGBT modeling works, we lean up on the Hefner physical model [7] which is classified among the first complete model with charge control [8] that shows excellent results in literature [9] and on the VHDL-AMS modeling works [10].

This model describes the n-channel IGBT as an n-channel MOSFET that supply the base current of the PNP bipolar transistor. Nevertheless, these internal components behave differently of their microelectronic counter-parts.

5.1. VDMOSFET CHARACTERISTICS

The expression of the current Imos crossing the VDMOSFET channel is described in literature [7]. Fig. 2 and 3 show the VDMOSFET capacitive elements. The Cgd capacitance is equal to the oxide capacitance Coxd for $\mathrm{Vds} \leq \mathrm{Vgs} - \mathrm{V_{Td}}$, for except that for $\mathrm{Vds} > \mathrm{Vgs} - \mathrm{V_{Td}}$, the Cgd capacitance will be constituted by a serial recombination of the Coxd capacitance and the depletion capacitance Cgdj at the level of the grid-drain overlap. The expression of this capacitance is described like follows:

- $V_{ds} \leq V_{gs} - \mathrm{V_{Td}}$
  $Cgd = \mathrm{Coxd}$
- $V_{ds} > V_{gs} - \mathrm{V_{Td}}$

$$Cgd = \frac{\mathrm{C_{oxd}} C_{gdj}}{\mathrm{C_{oxd}} + C_{gdj}} \quad (1)$$

$$Cgdj = \frac{\mathrm{A_{gd}} \varepsilon_{\mathrm{si}}}{Wgdj} \quad (2)$$

The sum of the oxide capacitance Coxs at the level of the grid-source overlap and the source metallization capacitance Cm forms the grid-source capacitance Cgs expressed by equation (3).

$$Cgs = \mathrm{Cm} + \mathrm{Coxs} \tag{3}$$

The depletion capacitance of the drain-source junction Cds is given by:

$$Cds = \frac{\mathrm{A_{ds}}\varepsilon_{\mathrm{si}}}{Wdsj} \tag{4}$$

The Cgd and Cds capacitances are also proportional to Agd and Ads surfaces with Wdsj and Wgdj are respectively the widths of the depletion zone for the drain-source and the grid-drain junctions.

5.2. BIPOLAR TRANSISTOR CHARACTERISTICS

Contrary to the conventional bipolar transistor, the base length is not anymore too small in relation to the diffusion length of its minority carriers. The transistor is thus separated to an anode-base junction, a base-cathode junction and a resistive base Rb. The equivalent diagram used for the IGBT modeling in VHDL-AMS is detailed on Fig. 2.

Contrary to the Iccer current that flows through the redistribution capacitance Ccer (6), the representation of the steady-state BJT collector current Icss doesn't depend on the variations of the anode-cathode potential. These two currents that flow through the transistor base are given by the following expressions:

$$Icss = \left(\frac{1}{1+\mathrm{b}}\right) I_T + \left(\frac{\mathrm{b}}{1+\mathrm{b}}\right)\frac{4\mathrm{D_p}}{W^2} Q \tag{5}$$

$$Iccer = Ccer\frac{dV_{ec}}{dt} \tag{6}$$

On the other hand, the anode-base junction is represented as a steady-state current Ibss set in parallel with the Iceb current. These currents are given by the following expressions:

$$Ibss = \frac{Q}{\tau_{\mathrm{HL}}} + \frac{Q^2}{Q_B^2}\frac{4N_{scl}^2}{\mathrm{n_i^2}} Isne \tag{7}$$

$$Iceb = \frac{dQ}{dt} \tag{8}$$

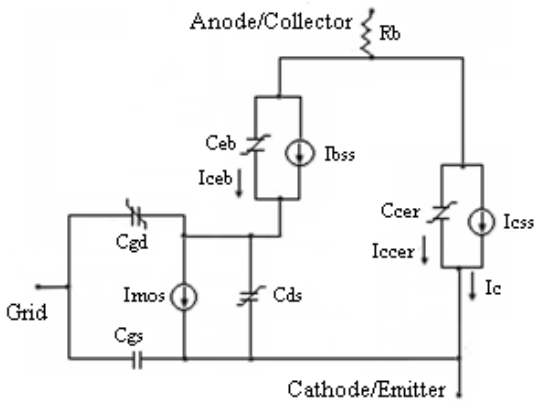

Fig. 2. Equivalent circuit model of the IGBT.

As we can see in Fig. 3, the VDMOSFET static operating regime is represented by the current generator Imos. The capacitance Cgs, Cgd and Cds reflect the charges storage in transistor and they intervene during the transient operation.

The Icss expression (5) consist of a non-quasi-static component due to the base electrons and holes transport coupling, and a charge-control component due to hole diffusion at hight-level injection conditions. The Ibss expression (7) consists of a recombination component and an electron injection component. So the Icss and the Ibss represent respectively the BJT collector and base current components that do not depend upon the time rate-of-change of the BJT base-collector and emitter-base voltage. In contrast, the current that flows through the BJT collector-emitter redistribution capacitance (6) depends on the time derivative of the capacitance voltage. Otherwise, the BJT emitter-base capacitance current (8) depends implicitly on the potential across the diffusion or the depletion capacitance [7].

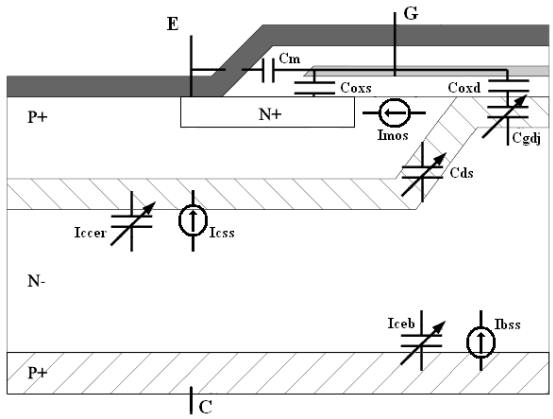

Fig. 3. Capacitive elements of an IGBT cell.

6. CONDUCTED EMI SIMULATION

As known, the main goal of the virtual prototyping is to reproduce a device functioning with adjustable levels of accuracy. Nonetheless, every semiconductor is considered as permanent or temporary carriers reservoir and its responses facing the external excitations depend of several physical constraints (non-linear behavior, temperature sensitivity…). These constraints become increasingly perplex in complex switches case (complex geometric structure, several doping level of the layers, elevated number of layers…) what makes the approximations taken at the behavioral modeling time a fatal source of errors on the electromagnetic perturbations analysis especially for the transient behavior. Those constraints justify our tendency to physical models for EMI simulation.

As a matter of fact, a physical model whose responses are highly accurate is essential to conduct an EMC study. The two main problems that appear when using physical models for semiconductor devices is the knowledge of the exact parameters needed to reproduce the real functioning of the device and the reduction of simulation time.

6.1. SIMULATION CIRCUIT TOPOLOGY

The different simulations presented in this survey have been done by using a buck converter circuit presented in Fig. 4. The switching cell is constituted of an IGBT transistor, a freewheeling diode and an inductive load.

To define the models parameters, we used the manufacturer's technical files [11]-[12] as a reference. The IGBT and the diode modeling can be achieved in an independent way since they represent two detached components in the same package [11] and it allows us to use the IGBT body diode as a freewheeling diode.

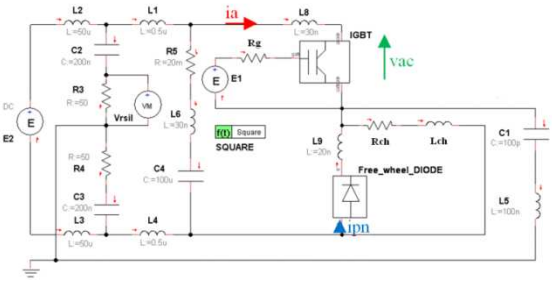

Fig. 4. Switching circuit.

At this phase of work, we referred to the literature [13]-[14] in order to approximate some IGBT parameters from the datasheet. The SGP30N60 IGBT already studied in the literature [10] was taken as a reference for our IGBT parameters since they have the same manufacturing technology and approximately the same characteristics. In further works, we will focus on the extraction and the adjustment of the parameters by an optimization approach in order to minimize the differences between the experimentations and simulations.

A LISN circuit has been inserted between the supply and the converter in order to calculate the conducted EMI generated by the circuit in both differential and common modes. The circuit was simulated with considering of the non-ideal electrical interconnections. In older works, we detailed the functioning of the switching cell by making a temporal analysis of the models responses [6].

The different simulations of these models are achieved on the Portunus® software. Conducted EMI versus time are extracted from the LISN. A simple Fast Fourier Transformation (FFT) calculation of these voltages allows us to deduce the EMI spectrum. These calculations were carried out on the Matlab® software.

6.2. EFFECT OF THE IGBT MODEL ON THE CONDUCTED EMI

During this observation we are interested in the amplitude variations that appear on the EMI spectrum which frequency band reaches 100 MHz. These variations are mainly due to the switching at the level of the non-linear components. Therefore, the frequencies and the amplitude of noise peaks could depend on some parameters of their models.

The duty cycle of the IGBT switching frequency is 0.5 generated by the control supply E1for a grid voltage included between 0V and 15V. The inductance of the load Lch is set to 200µH. The maximum step chosen for temporal sampling was 100ps.

In order to test the reliability of the IGBT model for the EMI simulation, we have varied the value of the grid resistance Rg (10Ω/60Ω), the load resistance Rch (30Ω/100Ω) for a fixed values of voltage source E2 (500V) and switching frequency (40kHz), then we observed the evolution of the conducted EMI at the LISN for each variation time. As shown in Fig. 5, the blue spectrum is gotten by using the already described IGBT model.

The variation of the grid resistance Rg proves that the switching time appears as an important factor for the spread spectrum. Also, the variation of the load resistance Rch proves the high current switching effect on high frequency current spike.

The major problem that we found during the conducted EMI extraction was the simulation time. The simulation time for 30µs of temporal representation at 40kHz of switching frequency was approximately 45 minutes to 55 minutes and for 60µs of temporal representation at 20kHz of switching frequency it largely exceeds 1 hour.

In order to reduce the simulation time, we focused on the dynamic behavior of the IGBT current during transient conditions. The BJT emitter-base current Iceb expressed in equation (8) represent the time rate-of-change of the base charge. The voltage that characterizes this junction is expressed by non-linear expressions and it describes implicitly its capacitance [7]. Contrary to the Iceb current, Iccer (6) depends on the non-linear redistribution capacitance Ccer times the time rate-of-change of the BJT emitter-collector voltage. As regard to the VDMOSFET, the currents that flow through the non-linear Cgd (1) and Cds (4) capacitances depend on the depletion widths and on the time rate-of-change of the junction's voltages. On the other hand, the current that flows through the static Cgs capacitance depends only on the time rate-of-change of the grid-source voltage.

With the purpose of minimizing the simulation time, we separated the static and the transient functioning of the IGBT model. In fact, since the Iccer, Icgd, Icds and the Icgs current are voltage time rate-of-change dependent, their major effect takes place during the switching phases, elsewhere their influences are minimal and can be neglected during the steady state behavior of the device.

In order to define the transition conditions from each state we are based on the value of the instantaneous excess carrier base charge Q and of the grid-source junction potential [1]. During the turn-on transition, the applied Vgs voltage exceeds the threshold voltage; the free carriers are injected from the BJT emitter to base region. Ones reaching the background mobile carrier base charge Qb, these free carriers will pass through the BJT base-collector junction or recombine with the electrons supplied from the MOS channel. Furthermore, since the doping concentration in the base is relatively low, the free carriers density is higher than the doping concentration which characterizes the state of high-level free carriers injection. So over this phase we have Q>Qb.

During the turn-off transition, no electrons current pass through the MOS channel and the IGBT behave like an open-base BJT. Subsequently, the anode current is only composed of the holes current due to the electrons-holes recombination and its decay time depends on free carriers life time in the base. Over this phase we can define Q included in [αQb>Qb, Qb] with α is an empirical value for the ratio Q/Qb. Beyond this, Q<Qb and thus the base doping concentration is much higher than the hole concentration until the next Vgs turning-on condition. As a conclusion, we can use these different statements to have an autonomous model able to detect its own transient instances.

The simplified model was implemented in the same circuit and tested at the same conditions as the original model. The red EMI spectrum is gotten after simplifying the model (Fig. 5). As we can see, the agreement between the two spectra validates the approximations imposed to simplify the initial model.

In low grid resistance case Rg (10Ω) we got the same results for the two models and for higher value of Rg (60Ω) the spectra are quite similar. The simplified model was also tested under other value of voltage source E2 (200V) and switching frequency (20kHz) and it also shows a very good agreement with the initial model. Furthermore, the simulation time for 30µs of temporal representation at 40kHz passed approximately to 7 minutes and to 8 minutes for 60µs of temporal representation at 20kHz.

At this level, the model does not consider the component thermal variations, but it does not prevent that the silicon temperature-dependent properties and the IGBT temperature-dependent parameters [15] could be taken into account even with the simplifications that we made.

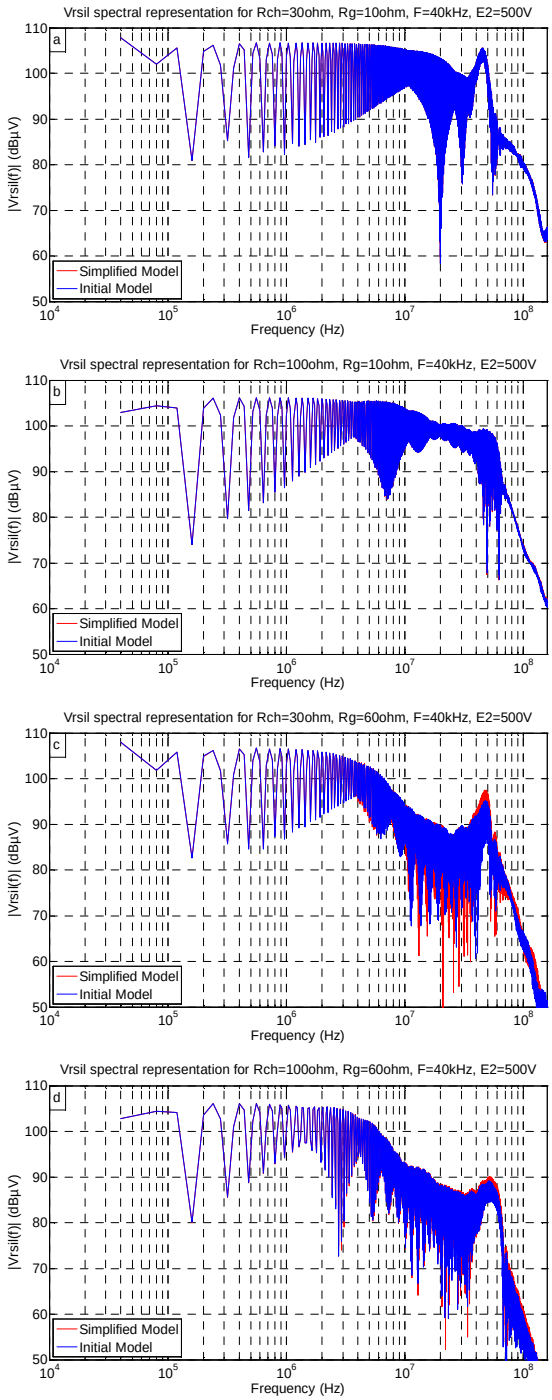

Fig. 5. EMI spectrum for F=40kHz and E2=500V. Rg=10Ω (a)Rch=30Ω, (b)Rch=100Ω Rg=60Ω (c)Rch=30Ω, (d)Rch=100Ω

These results allowed us to test the robustness of the IGBT model facing the external excitations, to show the considerable effect of semiconductor switching on EMI spectrums and in another step to identify the elements that mainly contribute to the resonances.

7. CONCLUSION AND PERSPECTIVES

The IGBT structure is similar to that of an n-channel VDMOSFET with the exception that the n-type drain contact is replaced by the p-type anode region for the IGBT. In contrast with microelectronic BJT, the internal IGBT epitaxial layer has a lightly doped wide base that add, compared to VDMOSFET, more complexity to the internal consideration of the bipolar phenomena which makes the modeling works, physical considerations and simplification efforts more prevalent and necessary in the case of bipolar components.

The EMI analysis at the conception stage of static converters circuits requires the use of accurate models for the semiconductor components. The previously developed physics-based IGBT model provides the basic criteria to lead off an EMC survey on a real prototype.

The model has been used to describe the different EMI spectra for various external circuit conditions. These preliminary results perform well for the range of static and dynamic conditions in which the device is intended to be operated. The validations of the proposed model in relation to experimental measurements are necessary at this stage.

8. REFERENCES

[1] Y. Yue, J. J. Liou, I. Batarseh, An Analytical Insulated-Gate Bipolar Transistor (IGBT) Model for Steady-State and Transient Applications Under All Free-Carrier Injection Conditions, Journal of Solid State Electronics, vol. 39, no. 9, pp. 1277–1282, Dec. 1996.

[2] Yisheng Yuan, Zhaoming Qian, An Improved Lumped-Charge Model and Parameter Extraction Approach of PIN Diodes, Power Electronics Specialists Conference, PESC ’02, 33rd Annual IEEE, November 2002.

[3] Francesco Iannuzzo, Giovanni Busatto, Physical CAD Model for High-Voltage IGBTs Based on Lumped-Charge Approach, IEEE Trans. Power Electronics, vol. 19, no. 4, pp. 885–893, July. 2004.

[4] Cliff L. Ma, P.O. Lauritzen, J. Sigg, Modeling of Power Diodes with the Lumped-Charge Modeling Technique, IEEE Trans. Power Electronics, vol. 12, no. 3, pp. 398–405, May. 1997.

[5] P.O Lauritzen, Compact Models for Power Semiconductor Devices, Tech.Rep. Available: http://www.ee.washington.edu/research/pemodels/. Last update: 19 November 2008.

[6] Slim Hrigua, Cyrille Gautier, Bertrand Revol, and François Costa, Using of VHDL-AMS to Model Power Semiconductors for EMI Simulation, Workshop 2emc, Rouen, France, 18-19 November 2010.

[7] Allen R. Hefner, Jr., Daniel M. Diebolt, An Experimentally Verified IGBT Model Implemented in the Saber Circuit Simulator, IEEE Trans. Power Electronics, vol. 9, no. 5, pp. 532–542, Sep. 1994.

[8] Serge Pittet, Modélisation Physique d’un Transistor de Puissance IGBT – Traînée en Tension à l’Enclenchement, Doctoral Thesis of the Federal Polytechnic School of Lausanne, Swiss, 2005.

[9] Allen R. Hefner, Jr., An Investigation of the Drive Circuit Requirements for the Power Insulated Gate Bipolar Transistor (IGBT), IEEE Trans. Power Electronics, vol. 6, no. 2, pp. 208–219, April. 1991.

[10] Their Ibrahim, Contribution au Développement de Modèles pour l’Électronique de Puissance en VHDL-AMS, Doctoral Thesis of the National Institute of the Applied Sciences of Lyon, France, 2009.

[11] Datasheet, IRG4PC40UD: Insulated Gate Bipolar Transistor with Ultrafast Soft Recovery Diode, International Rectifier.

[12] Datasheet, HFA15TB60/HFA15TB60-1: Ultrafast Soft Recovery Diode, Hexfred, Vishay.

[13] A.T. Bryant, X. Kang, E. Santi, P.R. Palmer, J.L. Hudgins, Two-Step Parameter Extraction Procedure With Formal Optimization for Physics-Based Circuit Simulator IGBT and p-i-n Diode Models, IEEE Trans. Power Electronics, vol. 21, no. 2, pp. 295–309, March. 2006.

[14] R. Chibante, A. Araújo, A. Carvalho, A Simple and Efficient Parameter Extraction Procedure for Physics Based IGBT Models, EPE-PEMC’04, Riga, Latvia, 2004.

[15] Allen R. Hefner, Jr., A Dynamic Electro-Thermal Model for the IGBT, IEEE Trans. Industry Applications, vol. 30, no. 2, pp. 394–405, Mar/Apr. 1994.